Selective Pharmacogenetic Activation of Catecholamine Subgroups in the Ventrolateral Medulla Elicits Key Glucoregulatory Responses

Ai-Jun Li,[1] Qing Wang,[1] and Sue Ritter[1]

[1]Programs in Neuroscience, Washington State University, Pullman, Washington 99164-7620

Catecholamine (CA) neurons in the ventrolateral medulla (VLM) contribute importantly to glucoregulation during glucose deficit. However, it is not known which CA neurons elicit different glucoregulatory responses or whether selective activation of CA neurons is sufficient to elicit these responses. Therefore, to selectively activate CA subpopulations, we injected male or female Th-Cre$^+$ transgenic rats with the Cre-dependent DREADD construct, AAV2-DIO-hSyn-hM3D(Gq)-mCherry, at one of four rostrocaudal levels of the VLM: rostral C1 (C1r), middle C1 (C1m), the area of A1 and C1 overlap (A1/C1), and A1. Transfection was highly selective for CA neurons at each site. Systemic injection of the Designer Receptor Exclusively Activated by Designer Drugs (DREADD) receptor agonist, clozapine-*N*-oxide (CNO), stimulated feeding in rats transfected at C1r, C1m, or A1/C1 but not A1. CNO increased corticosterone secretion in rats transfected at C1m or A1/C1 but not A1. In contrast, CNO did not increase blood glucose or induce c-Fos expression in the spinal cord or adrenal medulla after transfection of any single VLM site but required dual transfection of both C1m and C1r, possibly indicating that CA neurons mediating blood glucose responses are more sparsely distributed in C1r and C1m than those mediating feeding and corticosterone secretion. These results show that selective activation of C1 CA neurons is sufficient to increase feeding, blood glucose levels, and corticosterone secretion and suggest that each of these responses is mediated by CA neurons concentrated at different levels of the C1 cell group. **(*Endocrinology* 159: 341–355, 2018)**

Glucose is the obligatory substrate for brain energy metabolism; however, the brain itself stores very little glucose and depends on the delivery of glucose from the blood. Hence, the brain is equipped with mechanisms that detect glucose deficit and trigger coordinated systemic responses required to defend and replenish its glucose supply. These responses, referred to as counterregulatory responses (CRRs), activate behavioral, physiological, and endocrine systems that counter rapidly developing and profound glucose deficit and facilitate delivery of glucose to the brain (1). These protective responses include, among others, mobilization of stored glucose and fatty acids by adrenal medullary activation and glucagon secretion (2), replenishment of glucose by stimulation of feeding (3), increased gastric motility that facilitates digestion and absorption of ingested food (4), and increased corticosterone secretion that increases the usage of fatty acids, thereby decreasing peripheral glucose usage (5–9). CRRs are essential for survival. Pathological conditions in which they are impaired result in rapid neurologic deficit and can be lethal. Hypoglycemia-associated autonomic failure, a potential side effect of insulin treatment in diabetic individuals (1, 10), is an example of such a condition.

Several lines of investigation have established definitively that hindbrain catecholamine (CA) neurons are

ISSN Online 1945-7170

Received 12 July 2017. Accepted 18 October 2017.
First Published Online 24 October 2017

Abbreviations: 2DG, 2-deoxy-D-glucose; 5TG, 5-thioglucose; AAV, adeno-associated virus; AAV-hM3D, AAV2-DIO-hSyn-hM3D(Gq)-mCherry; CA, catecholamine; CART, cocaine- and amphetamine-regulated transcript; CNO, clozapine-*N*-oxide; CRR, counterregulatory response; DMM, dorsomedial medulla; DREADD, Designer Receptor Exclusively Activated by Designer Drugs; DBH, dopamine β-hydroxylase; DSAP, dopamine β-hydroxylase conjugated to saporin; IF, immunofluorescent; IML, intermediolateral column; ir, immunoreactive; NPY, neuropeptide Y; PBS, phosphate-buffered saline; PCR, polymerase chain reaction; PVH, paraventricular hypothalamus; Sub-P, subpostrema; TH, tyrosine hydroxylase; Th-Cre$^+$, Long Evans-Tg(Th-Cre)3.1; VLM, ventrolateral medulla.

necessary for elicitation of multiple CRRs to acute glucose deficit produced experimentally by insulin-induced hypoglycemia or systemic or central administration of the antiglycolytic drugs, 2-deoxy-D-glucose (2DG) and 5-thioglucose (5TG) (11–16). For example, selective ablation of CA neurons using the retrogradely transported immunotoxin, anti-dopamine β-hydroxylase (DBH) conjugated to the ribosomal toxin, saporin (DSAP) (17, 18), revealed that lesion of hindbrain CA neurons with projections to the hypothalamus eliminate glucoprivation-induced feeding (19) and elevation of corticosterone levels (13), modulation of growth hormone secretion (20), and suppression of estrous cycles (21). Retrograde lesions of CA neurons resulting from DSAP injections into the intermediolateral column (IML) of the spinal cord also established that spinally projecting CA neurons are necessary for glucoprivic control of adrenal medullary secretion (14, 19), a result later confirmed in rats in which DSAP was injected directly into the rostral subregion of the ventrolateral medulla (VLM), which houses cell bodies of spinally projecting CA neurons (22).

Despite strong evidence from various approaches that hindbrain CA neurons are necessary for elicitation of key CRRs, the specific phenotypes and characteristics of the CA neurons that mediate specific glucoregulatory responses are not known. Furthermore, it is not yet clear whether selective activation of distinct subpopulations of CA neurons in the VLM is sufficient to evoke specific CRRs. These questions have not been answered, in part, because of the anatomical complexity of the CA neurons themselves, including their collateralized projections, the apparent comingling of their functional subtypes, and the lack of technical approaches to overcome these obstacles. Therefore, in the present experiments, we used viral transfection of a Cre-dependent Designer Receptor Exclusively Activated by Designer Drugs (DREADD), a new technology that would enable selective activation of VLM CA neurons transfected at different rostrocaudal levels in Th-Cre$^+$ transgenic rats by systemic injection of clozapine-*N*-oxide (CNO), the synthetic agonist for the DREADD receptor (23). We tested the effects of selective CNO activation of CA neurons on corticosterone secretion, blood glucose, and food intake and on c-Fos expression in the VLM, dorsomedial medulla (DMM), hypothalamus, spinal cord, and adrenal medulla. To the best of our knowledge, our results show for the first time that selective pharmacogenetic activation of C1 neurons is sufficient to stimulate robust feeding, corticosterone, and blood glucose responses in the absence of glucoprivation and suggest a differential distribution of neurons mediating these specific responses within the C1 cell column. These results provide a foundation for further work to identify the specific neurons that mediate different CA responses to glucose deficit, how these responses are integrated to control emergency counterregulation, and how they participate in the overall control of metabolism.

Research Design and Methods

Animals

Male and female rats expressing Cre recombinase under the control of the tyrosine hydroxylase (TH) promoter [Long Evans-Tg(Th-Cre)3.1, or Th-Cre$^+$] and their wild-type non–Th-Cre (Th-Cre$^-$) littermates were used in these experiments (23). Transgenic rats were bred and raised in the Veterinary Biomedical and Research Building Vivarium at Washington State University from breeding stock generously provided by Dr. Karl Deisseroth (Stanford University, Stanford, CA).

The rats were maintained on a 12-hour light/12-hour dark cycle (lights on at 7 AM) with *ad libitum* access to pelleted rodent food (catalog no. 5001; LabDiet) and tap water. The Washington State University institutional animal care and use committee, which conforms to National Institutes of Health requirements, approved all experimental procedures.

Genotyping

Genotyping was performed at 3 weeks of age using polymerase chain reaction (PCR). One ear punch (1.0 mm in diameter) was heated at 95°C for 1 hour in 100 μL alkaline lysis buffer (15 mM NaOH/0.2 mM Na_2-EDTA $2H_2O$; pH, ~12). After mixing with 100-μL neutralization buffer (40 mM Tris-HCl; pH, ~5) and a 3-minute centrifugation, 4 μL of supernatant was used for PCR. PCR was performed in SYBR green buffer with a forward primer (5′-GCGGCATGGTGCAAGTTGAAT-3′) and a reverse primer (5′-CGTTCACCGGCATCAACGTTT-3′). The PCR cycles were 94°C for 3 minutes, 94°C for 20 seconds, 61°C for 20 seconds, and 72°C for 20 seconds for 35 cycles, followed by a melting curve reaction. A single production band was confirmed by gel electrophoresis and by a single melting curve peak at 86.5°C.

Targeted injection of DREADD virus into specific VLM sites

The CA cell groups in the hindbrain were defined using *The Rat Brain in Stereotaxic Coordinates* (24). Cell groups C1 and A1 are continuously distributed along the rostrocaudal extent of the VLM. Therefore, we adopted additional terms to subdivide these groups. We have referred to A1 as the portion of A1 caudal to overlap with C1 (from 14.9 to 14.2 mm, caudal to bregma). We have referred to the caudal portion of C1 overlapping the rostral portion of A1 as A1/C1 (from 14.1 to 13.4 mm, caudal to bregma). The middle portion of C1 is referred to as C1m (from 13.3 to 12.6 mm, caudal to bregma). The rostral portion of C1 is designated as C1r (from 12.5 to 11.8 mm, caudal to bregma). These areas were separately targeted for viral transfection in different groups of TH-Cre$^+$ and TH-Cre$^-$ rats. The parameters for accurate targeting of viral injections to each of these sites, including stereotaxic coordinates, injection volume, and the effectiveness and selectivity of the viral transfections for targeted CA neurons was determined before the main experiments (detailed in the Results section).

After completion of the preliminary studies, viral constructs were injected into 12- to 14-week-old male and 16- to 18-week-old female TH-Cre$^+$ rats and TH-Cre$^-$ male and female controls of the same age, as follows. A recombinant adeno-associated virus (AAV) containing a Cre-dependent doubly-floxed inverted open reading frame encoding and a reporter gene (mCherry) under a human synapsin I promotor, AAV2-DIO-hSyn-hM3D(Gq)-mCherry (AAV-hM3D), was injected into targeted sites along the rostrocaudal extent of the VLM CA cell column. Rats were anesthetized using 1.0 mL/kg of a ketamine/xylazine/acepromazine cocktail (50 mg/kg ketamine HCl; Fort Dodge Animal Health; 5.0 mg/kg xylazine; Vedco; and 1.0 mg/kg acepromazine; Vedco) and placed in a stereotaxic device. Two batches of virus (the titers were 2 and 4 $\times$ 10^{12} particles/mL; University of North Carolina Vector Core) were used during the experiment. No differences in transfection were found between these two batches in tests conducted before their use in the main experiments. The virus was injected as provided (without dilution) using a picospritzer through a pulled glass capillary pipette (30-μm tip diameter), bilaterally (200 nL/spot) into A1, A1/C1, C1m, or C1r in male rats. Pipettes were positioned dorsolaterally to the targeted site and directed medially at a 14° angle to avoid damage to, or transfection of, CA neurons in the nucleus of the solitary tract by potential diffusion of the viral construct along the pipette tract (Fig. 1). The following coordinates were used: 14.45 mm for A1, 13.75 mm for A1/C1, 12.95 mm for C1m, and 12.25 mm for C1r caudal to bregma: 4.0 to 4.1 mm lateral to the midline and 8.4 to 8.9 mm ventral to the skull surface (24).

In a separate experiment using female Th-Cre$^+$ rats, AAV-hM3D was unilaterally injected into both C1m and C1r (C1m+C1r AAV) in each rat to increase the distribution of the DREADD transcript in the VLM. Injections were performed unilaterally, rather than bilaterally as in the other groups, such that the total amount of virus injected into the VLM was equal across the groups.

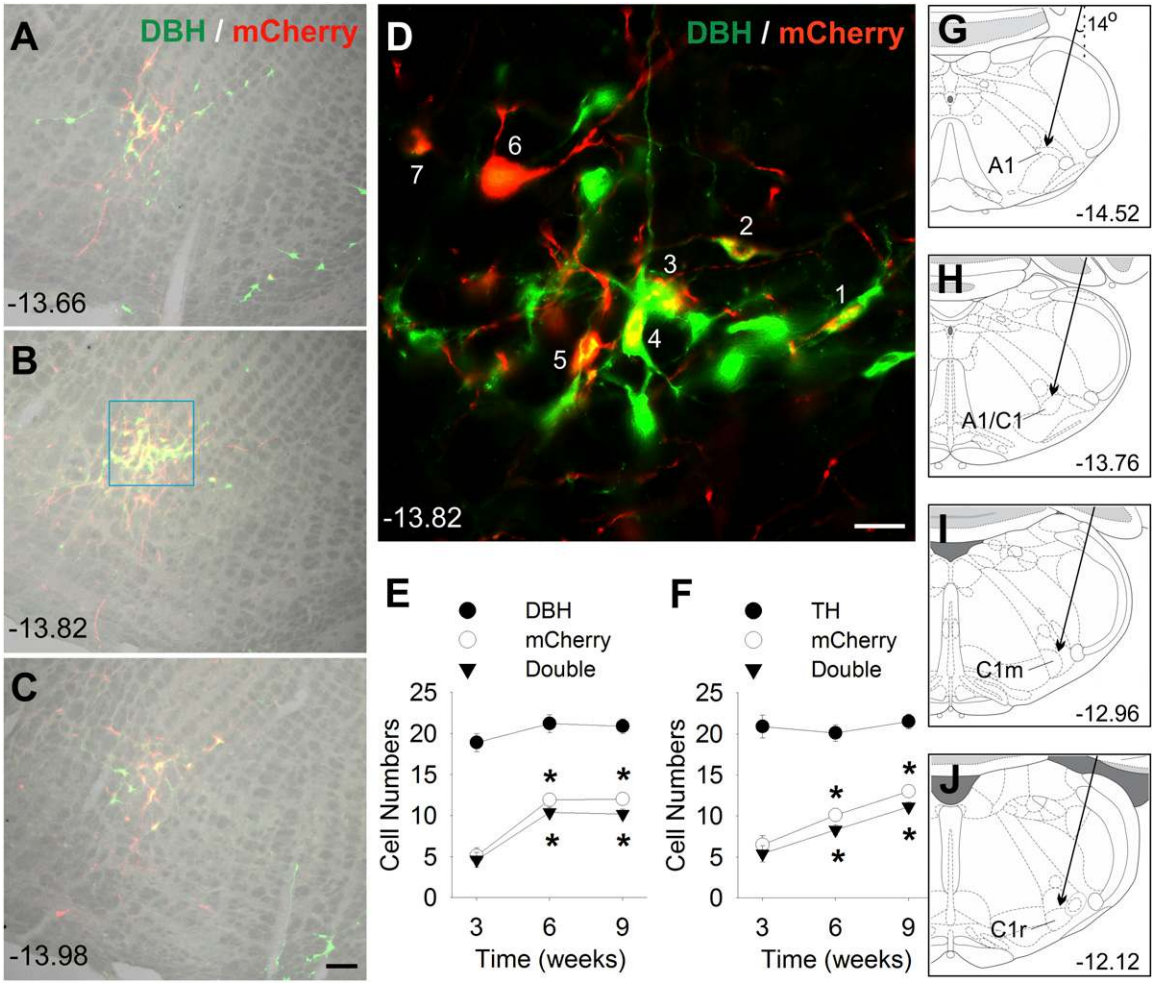

Figure 1. DBH/mCherry and TH/mCherry staining in A1/C1 region in Th-Cre$^+$ rats. (A–C) DBH/mCherry double staining in A1/C1 6 weeks after bilateral AAV-hM3D injection into A1/C1 of a female Th-Cre$^+$ rat. Merged images of bright-field image (gray) and double IF staining of DBH (green) and mCherry (red) at three rostrocaudal levels. (D) High-magnification IF image of DBH and mCherry of the area shown in the light blue square in B. All seven mCherry-positive cells (indicated by a number) in this image were also DBH-positive. Cell counts of (E) DBH/mCherry or (F) TH/mCherry staining in A1/C1 area at 3, 6, and 9 weeks after AAV-hM3D injection into A1/C1. Numbers were averages per side of 9 to 12 sections from three to four Th-Cre$^+$ rats (three sections per rat). *$P < 0.001$ vs values at 3 weeks (by *post hoc* Student-Newman-Keuls test after one-way analysis of variance). Scale bar = 100 μm in A to C and 25 μm in D. (A– D) Distance (in millimeters) caudal to bregma is shown. (G–J) Schematic drawings showing the target site for AAV injection into A1, A1/C1, C1m, and C1r regions, respectively. Arrows indicate the calculated trajectory of the glass capillary pipette inserted into VLM at a 14-degree angle. Distance (in millimeters) caudal to bregma, at approximately the middle of each injection site, is shown.

Measurement of food intake and blood glucose responses to systemic CNO and glucoprivation in VLM hM3D(Gq)-transfected rats

Responses to CNO were tested beginning 5 weeks after DREADD transfection. To activate hM3D(Gq) receptors, CNO (Tocris) was dissolved in sterile saline (0.9%) and injected at a dose of 1 mg/kg intraperitoneally. The antiglycolytic drug, 2DG (Sigma-Aldrich), was dissolved in sterile saline and injected at a dose of 250 mg/kg subcutaneously to induce glucoprivation (19). Food intake was measured in a 4-hour test after injection of CNO, 2DG, or the saline (0.9%) vehicle at 9:30 AM in 1-hour–fasted rats. Blood glucose concentrations were measured in the absence of food before and during a 4- or 6-hour period after the drug injections at 10:30 AM in 2-hour–fasted rats. Glucose was measured from tail blood using a GlucoCard Vital glucose meter (Arkray). All tests were performed 5 to 9 weeks after the AAV injections, when transfection was stably expressed. Individual tests were separated by ≥3 days.

Jugular catheter implantation, blood sampling, and enzyme-linked immunosorbent assay for measurement of corticosterone

Separate groups of male rats, transfected at the same sites, as described for feeding and blood glucose testing ($A1^{AAV\text{-}hM3D}$, $A1/C1^{AAV\text{-}hM3D}$, $C1m^{AAV\text{-}hM3D}$, $C1r^{AAV\text{-}hM3D}$), were prepared for analysis of CNO- and 2DG-induced corticosterone secretion. To minimize handling stress during sample collection for corticosterone measurement, these rats were implanted with chronic jugular catheters for remote blood collection. The catheter, made of Silastic tubing (inside diameter, 0.64 mm; outside diameter, 1.19 mm; Dow Corning), was implanted into the atrium through the right jugular vein under anesthesia induced by the ketamine/xylazine/acepromazine cocktail (13). As in the other groups, the tests were performed 5 to 9 weeks after stereotaxic DREADD transfection. The catheters were implanted ~1 week before the collection of blood for corticosterone determination. After recovery, the rats were habituated to 30-cm × 10-cm opaque Plexiglas chambers, which were used for the remote blood sampling. On test days, 2-hour–fasted rats were placed in the chambers, and the blood samples (~300 μL) were collected remotely at several time points before and after each treatment. After clotting for 1 to 2 hours at 4°C and centrifugation, the serum samples were stored at −80°C (25). The plasma corticosterone levels were measured with a mouse/rat corticosterone enzyme-linked immunosorbent assay kit (catalog no. IB79175; IBL America), according to the provided instructions.

Immunohistochemistry

After completion of behavioral tests (8 to 10 weeks after AAV-hM3D injection), the rats were deprived of food for 2 hours and injected with CNO (1 mg/kg intraperitoneally) or saline. Two hours later, they were euthanized by deep isoflurane-induced anesthesia (Halocarbon Products). Just before cessation of the heartbeat, the rats were perfused transcardially with phosphate-buffered saline (PBS; pH 7.4) followed by freshly made 4% formaldehyde/PBS solution. The brain, adrenal medulla, and spinal cord were rapidly removed and placed in 4% formaldehyde/PBS for 5 hours, followed by immersion in 25% sucrose in PBS overnight (16 hours) and then sectioned with a cryostat at 40-μm thickness. Coronal brain sections for hindbrain and hypothalamus (four serial sets), sagittal spinal cord sections (one set), and adrenal medullary sections (two sets) were collected for analysis of the distribution and selectivity of DREADD transfection and for c-Fos expression induced by CNO.

For double or triple immunofluorescent (IF) staining, the sections were incubated with primary antibodies at 4°C for 2 days in 10% normal horse serum/PBS, washed, and incubated in secondary antibodies for 4 hours (26, 27). The following antibodies were used: mouse anti-mCherry (ClonTech Laboratories), rabbit anti-DsRed (ClonTech Laboratories; for detecting mCherry); rabbit anti-TH (Millipore); mouse anti-DBH (Millipore); goat anti–c-Fos (Santa Cruz Biotechnology) and donkey anti-mouse, donkey anti-rabbit, or donkey anti-goat antibody conjugated with Alexa Fluor 488, Cy3, or Alexa Fluor 647 (all 1:500 dilution in 1% normal horse serum/Tween PBS; Jackson ImmunoResearch). The sections were mounted and coverslipped with ProLong Gold medium (ThermoFisher Scientific) and observed and photographed using a Zeiss epifluorescent or Leica confocal microscope.

For c-Fos staining in the adrenal medulla and spinal cord, standard avidin-biotin-peroxidase methods were used. The sections were incubated with goat anti–c-Fos antibody (1:5000) for 2 days, followed by overnight incubation in biotinylated donkey anti-goat IgG (1:500; Jackson ImmunoResearch) and a 4-hour incubation in ExtrAvidin-peroxidase (1:1500; Sigma-Aldrich). Nickel-intensified diaminobenzidine was used to produce a gray/black reaction product by peroxidase reaction (27, 28).

Neuroanatomical analysis and quantification of results

A virus injection was considered to be targeted accurately if mCherry expression was contained within one of our defined VLM subdivisions (see the Research Design and Methods section). Typically, each defined target zone was composed of four to five tissue coronal sections. For quantification in rats with bilateral single-site injections, DBH-, TH-, mCherry-, and c-Fos–positive cells were counted bilaterally in each rat from the three coronal sections within the targeted zone containing the most abundant mCherry signal. In rats with injections at two adjacent sites (C1r+C1m), labeled cells were counted from seven coronal sections containing the most abundant mCherry signal.

The DMM also contains CA neurons. These cells are distributed in cell groups A2 in the caudal DMM and C2 in the rostral DMM. Although our pipettes were angled to avoid traversing these areas, we nevertheless examined the DMM in the experimental rats to identify any cells that might have been inadvertently transfected by the DREADD construct and to identify areas of c-Fos expression. Cells in A2, subpostrema (Sub-P), and dorsolateral solitary nucleus were examined and counted (two sections per rat) at 13.9 to 13.7 mm or 14.4 to 14.2 mm (for Sub-P), caudal to bregma.

Two sites innervated by VLM CA neurons, the paraventricular hypothalamus (PVH) and the IML of the thoracic spinal cord were also examined for c-Fos expression in response to CNO in the VLM transfected rats. This was done to verify that CNO activation of VLM sites produced the expected activation of the VLM CA projection sites. In addition, c-Fos expression in the adrenal medulla, which is innervated by preganglionic neurons in the IML, was assessed. Positive cells in the PVH were counted bilaterally from three sections per rat (at

1.5 to 1.9 mm, caudal to bregma). IML and adrenal medullary c-Fos expression were not quantified.

Statistical analysis

All results are presented as the mean ± standard error of the mean. For statistical analysis of the data, we used the unpaired *t* test and one-way or two-way repeated-measures analysis of variance, as appropriate. After statistical significance was determined by analysis of variance, multiple comparisons between individual groups were tested using a *post hoc* Student-Newman-Keuls test. $P < 0.05$ was considered to indicate statistical significance.

Results

Time course, selectivity, and localization of mCherry reporter gene expression in VLM CA neurons: preliminary experiments

Preliminary experiments were conducted to determine the final protocols for the main experiments. The efficacy, specificity, and time course of hM3D(Gq) expression in CA neurons were investigated using double IF staining of the reporter gene mCherry plus DBH or TH in female Th-Cre$^+$ rats after bilateral AAV-hM3D injection into A1/C1. Both CA-directed antibodies produced similar results. Using standard microscopy (Fig. 1), 24% to 26% of DBH- or TH-immunoreactive (ir) neurons in A1/C1 were mCherry-positive 3 weeks after AAV injection. At 6 and 9 weeks, 41% to 49% of CA neurons were mCherry-positive, 84% and 89% of mCherry-positive cells were DBH-ir, and 82% and 89% were TH-ir. More sensitive analysis using confocal images at 6 weeks revealed that almost all (93%) mCherry-ir cells were CA neurons. The rostrocaudal extent of mCherry expression at each injection site was 0.50 ± 0.02 mm in these rats. In contrast, female control Th-Cre$^-$ rats with AAV-hM3D injected unilaterally into A1/C1 showed no mCherry-ir cells at 8 weeks after virus injection in either the injected or noninjected side of the VLM.

Similar transfection rates were confirmed in the males. Male Th-Cre$^+$ rats with AAV-hM3D injection in A1/C1 showed similar mCherry transfection rates at both 5 and 10 weeks (~50%; see also later paragraphs for details) that were similar to those of female rats at 6 or 9 weeks (see previous paragraph). Together, these preliminary results indicated effective and selective mCherry expression in CA neurons. No mCherry-positive cell bodies were found in any area outside of the VLM in either the male or female rats (three to five rats per sex). No sex-related differences were found in the extent of virus transfection in female and male Th-Cre$^+$ rats in these studies. Based on these preliminary results, the responses to systemic CNO injection were tested in the main experiments 5 to 9 weeks after AAV injection when mCherry expression was stable.

Effects of pharmacogenetic activation of CA neurons on feeding, blood glucose, and corticosterone secretion

The effects of selective CNO-induced activation of CA neurons on feeding and blood glucose were investigated in male Th-Cre$^+$ rats after bilateral AAV-hM3D injection into A1, A1/C1, C1m, or C1r (Fig. 2). CNO injection (1 mg/kg) significantly increased the 2-hour and 4-hour food intake compared with the intake after saline injection in A1/C1$^{\text{AAV-hM3D}}$, C1m$^{\text{AAV-hM3D}}$, and C1r$^{\text{AAV-hM3D}}$ rats but not in A1$^{\text{AAV-hM3D}}$ rats. The magnitude and time course of the feeding response was comparable at all three positive sites to the response induced by 2DG (250 mg/kg) in the same rats. However, injection of the same dose of CNO that stimulated food intake did not change the blood glucose levels in these same rats, although the blood glucose levels were significantly increased in these rats by 2DG injection (Fig. 2).

Changes in the plasma corticosterone levels in the rats transfected with AAV-hM3D in A1, A1/C1, C1m, and C1r were measured in a separate group of male rats after saline, 2DG (250 mg/kg), or CNO (1 mg/kg) injection (Fig. 2). CNO increased the corticosterone levels most effectively in the A1/C1- and C1m-transfected rats, increased corticosterone only slightly in the C1r-transfected rats, and did not increase corticosterone in the A1-transfected rats. The effects of 2DG and CNO on food intake and blood glucose at the four injection sites in this group of rats were similar to those shown for the previous group (data not shown).

Evaluation of DREADD transfection and pharmacogenetic activation of VLM c-Fos expression

At 8 to 10 weeks after injection of AAV-hM3D into the VLM subregions (~1 week after testing was complete), the rats were treated with CNO (1 mg/kg) or saline and prepared for anatomical evaluation of viral transfection selectivity and distribution and CNO-induced c-Fos expression (Fig. 3). The specificity of mCherry expression in CA neurons was investigated by double IF staining of DBH and mCherry. The expression of mCherry was limited to the targeted site. Figure 3(A) shows the extent of the viral transfection along the rostrocaudal axis of the VLM for each targeted site. Labeling extended 0.62 ± 0.05 mm, 0.66 ± 0.06 mm, 0.77 ± 0.08 mm, and 0.64 ± 0.06 mm rostrocaudally along the VLM for A1$^{\text{AAV-hM3D}}$, A1/C1$^{\text{AAV-hM3D}}$, C1m$^{\text{AAV-hM3D}}$, and C1r$^{\text{AAV-hM3D}}$ rats, respectively. Supplemental Figs. 1 through 4 show the distribution of mCherry-labeled neurons for each of the four targeted VLM levels from two representative rats from each target group. Cell counting revealed that 53.9% ± 1.9%, 49.9% ± 1.9%, 53.5% ± 1.9%, and 48.6% ± 2.9% of DBH-ir neurons were mCherry-positive

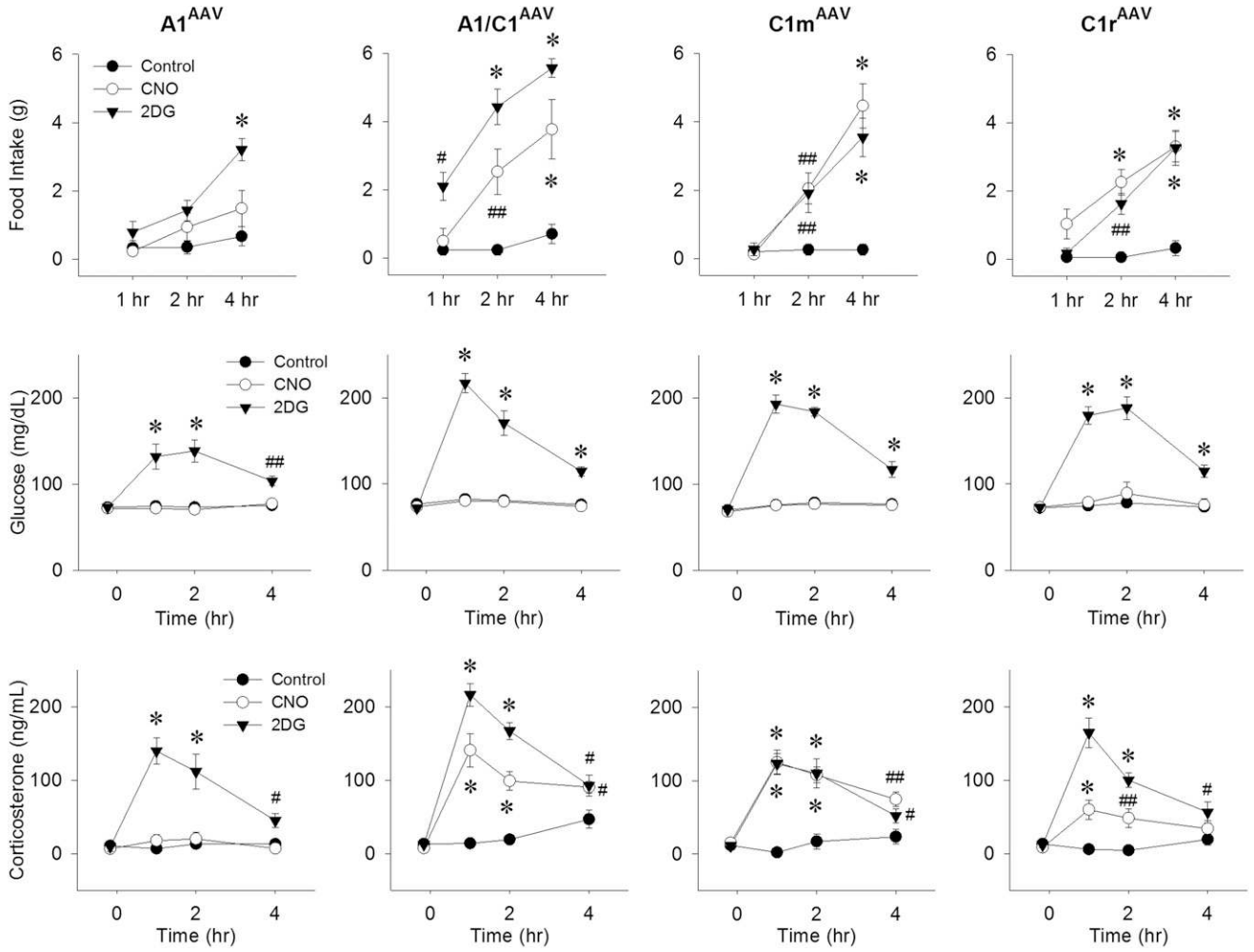

Figure 2. Food intake, blood glucose, and corticosterone levels in Th-Cre$^+$ rats after CNO injection. Responses during the 4-hour period after control (0.9% saline intraperitoneally), CNO (1 mg/kg intraperitoneally), or 2DG (250 mg/kg subcutaneously) injection in male Th-Cre$^+$ rats given bilateral AAV-hM3D injections into A1, A1/C1, C1m, or C1r, respectively. (Upper) Food intake; (middle) blood glucose levels in the absence of food; and (lower) plasma levels of corticosterone. $^{\#}P < 0.05$; $^{\#\#}P < 0.01$; $^{*}P < 0.001$ vs saline control at the same time points by *post hoc* Student-Newman-Keuls test after two-way repeated-measures analysis of variance (six to eight rats for each treatment).

in A1$^{\text{AAV-hM3D}}$, A1/C1$^{\text{AAV-hM3D}}$, C1m$^{\text{AAV-hM3D}}$, and C1r$^{\text{AAV-hM3D}}$ rats, respectively (Fig. 3D). CNO injection dramatically increased c-Fos expression in virus-transfected CA neurons (Fig. 3B–3E). Double IF staining with c-Fos/mCherry indicated that 78.2% ± 2.9%, 84.9% ± 1.6%, 90.5% ± 1.8%, and 81.6% ± 1.8% of mCherry-labeled neurons were activated in the injection site in A1$^{\text{AAV-hM3D}}$, A1/C1$^{\text{AAV-hM3D}}$, C1m$^{\text{AAV-hM3D}}$, and C1r$^{\text{AAV-hM3D}}$ rats, respectively (Fig. 3B and 3D). Triple IF staining for DBH/c-Fos/mCherry demonstrated that most c-Fos–positive cells (86.5%, 90.2%, 84.7%, and 90% in A1$^{\text{AAV-hM3D}}$, A1/C1$^{\text{AAV-hM3D}}$, C1m$^{\text{AAV-hM3D}}$, and C1r$^{\text{AAV-hM3D}}$ rats, respectively) were triple labeled (Fig. 3C and 3E).

Histological analysis revealed 4 rats (from a total of 65 rats) in which injections of the AAV-hM3D construct were apparently "off-target." Because they produced no evidence of transfection at any site, these injections had undoubtedly been delivered into non-CA areas, most likely dorsal to the target site. None of these rats responded to CNO; however, they did show typical responses to 2DG, such as shown for the control rats. These data were not included in the statistical analyses, because the injection site could not be determined.

CNO-induced c-Fos expression in DMM and PVH

Activation of neurons in the DMM by CNO-induced stimulation of A1 and C1 neurons was also examined. mCherry-positive fibers, but no mCherry-positive cell bodies, were found in the DMM (Fig. 4A–4F and 4H) in any of the AAV-transfected rats, confirming the selectivity of transfection for VLM-targeted sites. In A1$^{\text{AAV-hM3D}}$, A1/C1$^{\text{AAV-hM3D}}$, C1m$^{\text{AAV-hM3D}}$, C1r$^{\text{AAV-hM3D}}$, and C1m+C1r$^{\text{AAV-hM3D}}$ transfected rats, c-Fos was found in limited regions of the nucleus of the solitary

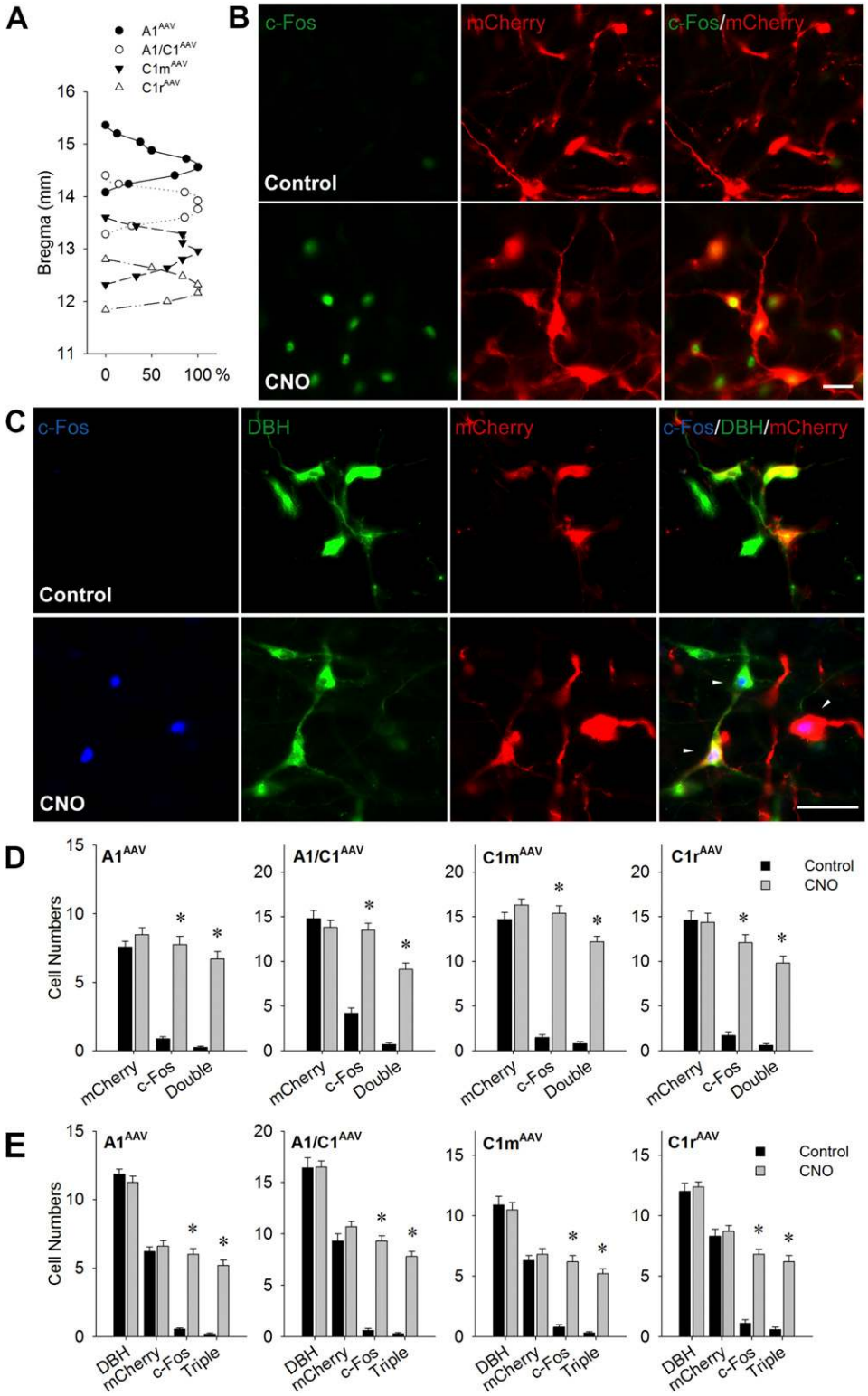

Figure 3. CNO-induced c-Fos expression in VLM in rats euthanized 2 hours after saline or CNO injection (1 mg/kg intraperitoneally) in the absence of food. (A) Distribution of mCherry expression in VLM in rats transfected with AAV-hM3D at A1, A1/C1, C1m, and C1r, shown as the percentage of rats with ≥5 mCherry-positive cells per side at each bregma level. Distance caudal to bregma is shown on the *y*-axis. (B) Representative double IF images of c-Fos (green) and mCherry (red) in the A1/C1 area of male A1/C1$^{AAV\text{-}hM3D}$ Th-Cre^{+} rats. Scale bar = 25 μm. (C) Representative triple IF staining of c-Fos (blue), DBH (green), and mCherry (red) in C1m area in male C1m$^{AAV\text{-}hM3D}$ Th-Cre^{+} rats. White triangles indicate triple-stained cells in CNO-treated rats. Scale bar = 25 μm. Cell counts of c-Fos–positive cells in VLM catecholamine regions at the AAV injection site by (D) double or (E) triple staining. Numbers of cells with positive staining in the targeted A1, A1/C1, C1m, or C1r, respectively, of male Th-Cre^{+} rats injected bilaterally with AAV-hM3D. Numbers are averages per site using 9 to 12 sections from three to four rats (three sections per rat). *$P < 0.001$ vs saline-injected control by unpaired *t* test.

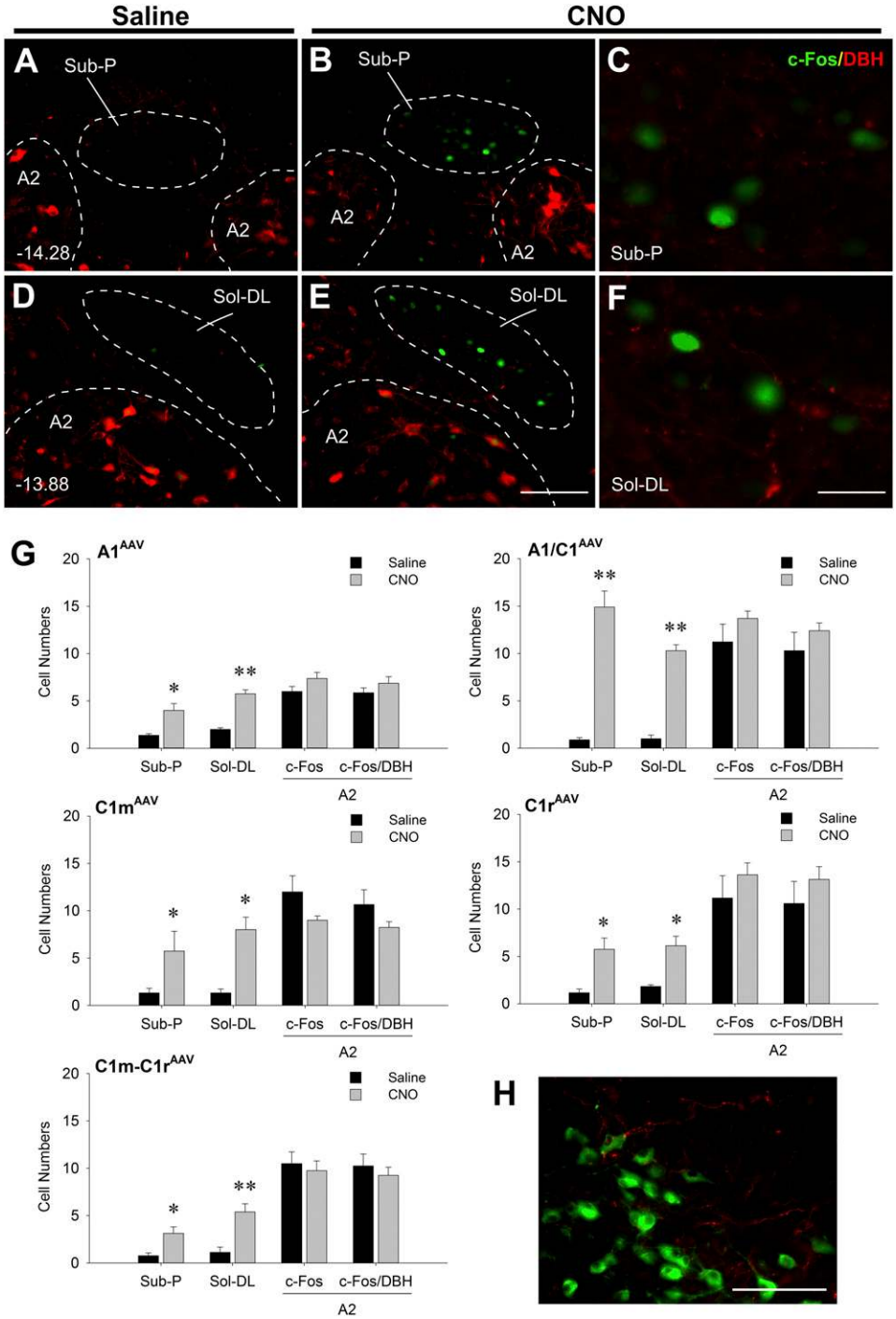

Figure 4. Expression of c-Fos, DBH, and mCherry in DMM of Th-Cre^{+} rats virally transfected in the VLM and euthanized 2 hours after saline or CNO injection (1 mg/kg intraperitoneally) in the absence of food. (A–F) Representative double IF images at two rostrocaudal levels of the DMM showing c-Fos (green) and DBH (red) in DMM in A1/C1$^{AAV\text{-}hM3D}$ rats. (C and F) High magnification of areas in (B) and (E) showing strong c-Fos expression and surrounding DBH terminal staining, respectively. Distances (in millimeters) caudal to bregma are shown in (A) and (D). Scale bar = 100 μm (for A, B, D, and E). Scale bar = 25 μm (for C and F). (G) Cell counts of c-Fos and c-Fos/DBH in Sub-P area, solitary nucleus, dorsolateral region (Sol-DL), and A2 regions in A1$^{AAV\text{-}hM3D}$, A1/C1$^{AAV\text{-}hM3D}$, C1m$^{AAV\text{-}hM3D}$, C1r$^{AAV\text{-}hM3D}$, and C1m+C1r$^{AAV\text{-}hM3D}$ rats. Numbers are averages of 6 to 10 sections from three to five rats (two sections per rat). $*P < 0.01$; $**P < 0.001$ vs saline-injected control (by unpaired *t* test). (H) A representative double IF image of DBH (green) and mCherry (red) in DMM in a C1m$^{AAV\text{-}hM3D}$ rat showing mCherry-positive fibers and the absence of mCherry-positive cell bodies in A2 and Sol-DL. Scale bar = 100 μm.

tract, especially in areas just ventral to the fourth ventricle (*i.e.*, in the Sub-P and dorsolateral solitary nucleus) after CNO treatment. In these two regions, A1/C1$^{AAV\text{-}hM3D}$ transfected rats expressed higher numbers of c-Fos–ir neurons than did the rats transfected at any of the other C1 sites. Double IF staining with DBH revealed that these CNO-activated neurons were non-CA neurons (Fig. 4G).

CNO increased c-Fos expression in the PVH in A1/C1$^{AAV\text{-}hM3D}$ and C1m$^{AAV\text{-}hM3D}$ rats (Fig. 5), the only rats in which PVH c-Fos was examined. This increased activation of PVH is consistent with our previous report (27), with CNO-induced elevation of plasma corticosterone levels and strong expression of mCherry fibers in PVH in the present study and activation of CA neurons known to innervate the PVH (29, 30).

Effects of pharmacogenetic activation of C1m plus C1r neurons on feeding, blood glucose, and c-Fos expression in IML and adrenal medulla

In this experiment, AAV-hM3D was unilaterally injected into both C1m and C1r in female Th-Cre$^+$ rats. As shown in Fig. 6A and 6B, CNO injection (1 mg/kg) increased both food intake and blood glucose in dual-transfected rats to levels roughly equivalent to those produced in the same rats by systemic 2DG injection (250 mg/kg). Female rats transfected at C1m+C1r did not differ from males with respect to food intake when intake was corrected for differences in body weight. At the time of the feeding tests, the body weight of the females was 61.0% ± 1.3% that of the males' weight, and the food intake of the females was 60.6% ± 9.2% that of the males' intake (data included saline, 2DG, and CNO tests for A1-, A1/C1-, C1m-, and C1r-transfected male rats).

Dual transfection of both C1m and C1r produced more extensive mCherry expression in rostral and middle C1 than when separate injections were made into each single site. The rostrocaudal extent of mCherry expression was 1.32 ± 0.08 mm in these rats (Fig. 6E; Supplemental Fig. 5). Similarly, 58.4% ± 2.4% of DBH-ir neurons near the injection sites were mCherry-positive. Expression of c-Fos in C1m+C1r regions was significantly increased by CNO injection compared with control saline injection (Fig. 6C and 6D). Double staining revealed that most (86.5% ± 1.0%) mCherry-ir cells were c-Fos–positive. Triple IF staining of c-Fos/mCherry/DBH confirmed that 84.6% of mCherry/DBH cells were activated by CNO treatment. In contrast to rats with single transfection sites, CNO increased c-Fos expression in the IML cell column at thoracic segments T5 to T10 and in the adrenal medulla in rats with dual transfection of C1m+C1r (Fig. 7), consistent with the stimulation of a hyperglycemic response in these rats.

Discussion

Injection of Cre-dependent AAV-hM3D-mCherry into the C1 or A1 cell group in Th-Cre$^+$ transgenic rats produced a selective and effective transfection of CA neurons at each injection site. In Th-Cre$^+$ rats, virtually all the mCherry-labeled cells at the injection sites were CA neurons, and no mCherry-labeled cells were present in non–Th-Cre (Th-Cre$^-$) rats. Furthermore, we found no evidence of transfection of cell bodies in CA cell groups outside the VLM (A2, A5, C2, C3) after C1 or A1 injections in TH-Cre$^+$ rats. These observations support our conclusion that responses to CNO resulted from activation of DREADD constructs expressed in A1 and C1 and not from DREADD activation of other CA cell groups.

Activation of the transfected A1 and C1 neurons after systemic CNO injections evoked robust behavioral, autonomic, and endocrine responses that were similar in magnitude and time course to those elicited by systemic 2DG. Double staining for c-Fos and mCherry immunoreactivity revealed that most (78% to 91%) of c-Fos–ir neurons were also mCherry-immunopositive, and triple IF staining (c-Fos/mCherry/DBH) confirmed that 85% to 90% of mCherry/DBH cells were activated by CNO treatment. These anatomical results indicate that the CNO-induced feeding, corticosterone, and blood glucose responses we observed in this experiment resulted from activation of CA neurons in the VLM (and most likely in C1), indicating that selective activation of these CA neurons is sufficient to elicit critical glucoregulatory responses even in normoglycemic rats.

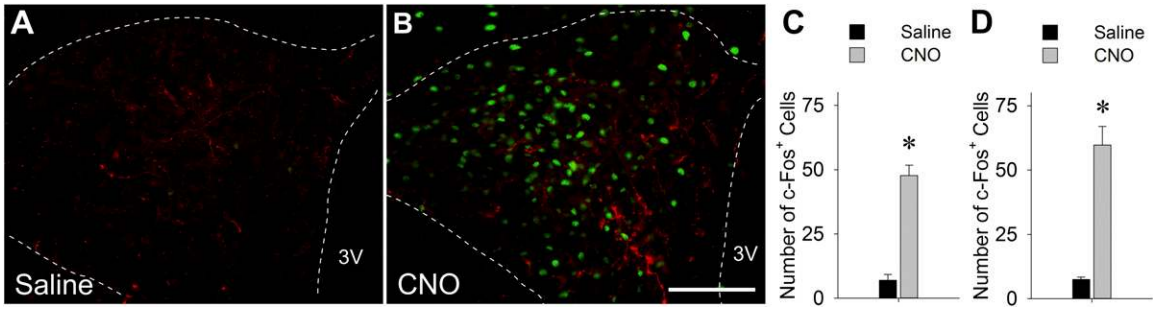

Figure 5. Expression of c-Fos in PVH. (A, B) Representative double IF staining of c-Fos (green) and mCherry (red) in PVH of C1m$^{AAV\text{-}hM3D}$ rats 2 hours after saline or CNO injection (1 mg/kg intraperitoneally). Scale bar = 100 μm. Numbers of cells expressing c-Fos in PVH in (C) A1/C1$^{AAV\text{-}hM3D}$ transfected rats and (D) C1m$^{AAV\text{-}hM3D}$ transfected rats. Data show averages of the counts from both sides from five rats per treatment (three sections per rat). *$P < 0.001$ vs saline-injected control (by unpaired t test). 3V, third ventricle.

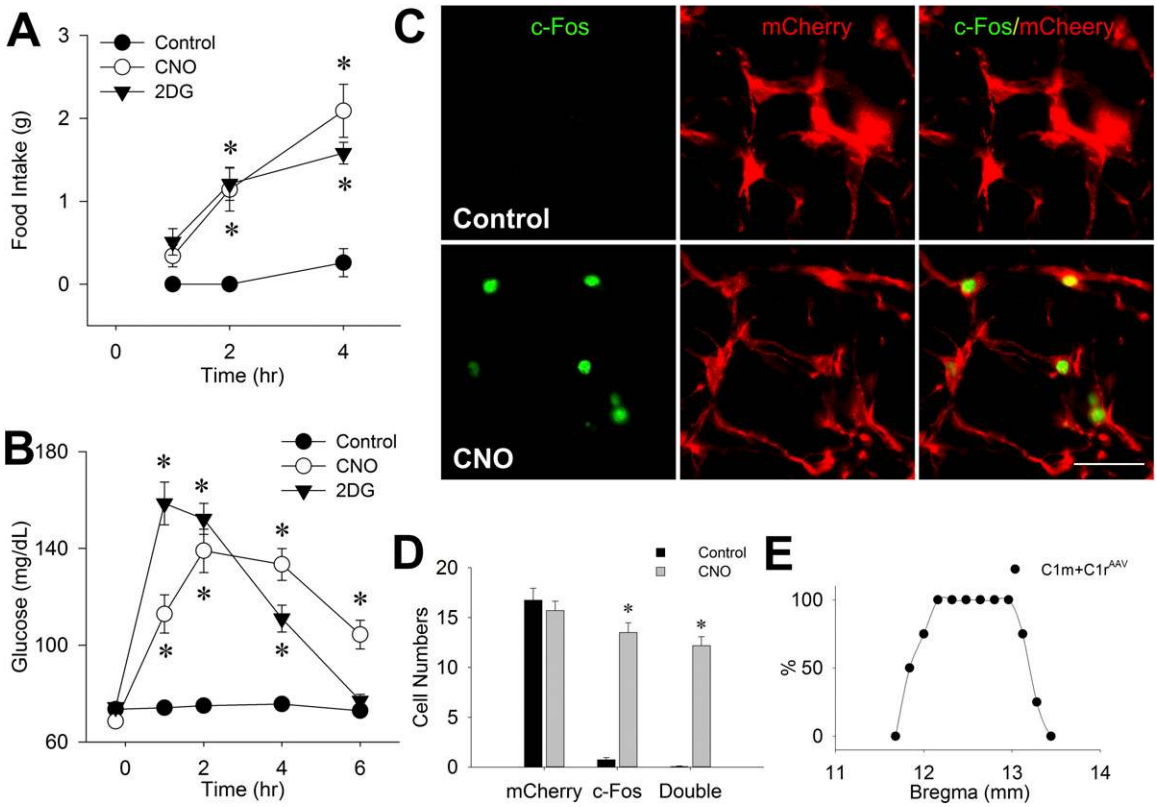

Figure 6. Food intake, blood glucose, and c-Fos expression in VLM after CNO injection in C1m+C1r$^{AAV\text{-}hM3D}$ rats. (A) Food intake and (B) blood glucose levels during the 4-hour (for feeding) or 6-hour (for glucose) period after control (intraperitoneal saline), 2DG (250 mg/kg subcutaneously), or CNO (1 mg/kg intraperitoneally) administration in female Th-Cre^{+} rats injected unilaterally with AAV-hM3D into both C1m and C1r (n = 8 rats per treatment). *$P < 0.001$ vs saline control at the same time point (by *post hoc* Student-Newman-Keuls test after two-way repeated-measures analysis of variance). (C) Representative double staining of c-Fos (green) and mCherry (red) in female C1m+C1r$^{AAV\text{-}hM3D}$ Th-Cre^{+} rats 2 hours after saline (control) or CNO (1 mg/kg intraperitoneal) injection. Scale bar = 25 μm. (D) Cell numbers of c-Fos/mCherry in C1m+C1r averaged from three to four rats (seven sections per rat). *$P < 0.001$ vs saline-injected control (by unpaired *t* test). (E) Distribution of mCherry expression in VLM, expressed as percentage of rats with ≥5 mCherry-positive cells per site at each bregma level in C1m+C1r$^{AAV\text{-}hM3D}$ Th-Cre^{+} rats. Distance caudal to bregma is shown on *x*-axis.

As the sole mechanism for replenishment of depleted glucose reserves, increased food intake is of obvious importance as a CRR. Previous results indicated that hindbrain CA neurons that project to the hypothalamus are necessary for increased food intake in response to glucoprivation. Selective retrograde ablation of hypothalamically projecting CA neurons, resulting from PVH or lateral hypothalamic immunotoxin injection, permanently abolish glucoprivic feeding (19, 26), without apparent disruption of other controls of food intake or the ability of lesioned rats to maintain body weight under *ad libitum* feeding conditions (19). Most of the rostral projecting A1/C1 neurons co-express neuropeptide Y (NPY) and selective co-silencing of DBH and NPY genes in A1/C1 also attenuates feeding in response to systemic glucoprivation (2DG) (28). Nevertheless, because injection of DSAP into PVH damages CA neurons in the dorsal and ventral medulla (13, 19), the sufficiency of ventral medullary CA neurons to increase food intake has remained uncertain. However, the results we have presented clearly show that selective CNO activation is sufficient to increase food intake at each of the DREADD transfection sites along the entire longitudinal extent of the C1 cell group. Importantly, although many CA neurons throughout the A1 and the C1 cell group are activated by glucose deficit (11, 31), food intake was not evoked by DREADD activation of A1 caudal to its overlap with C1. Hence, our results strongly suggest that the neurons that mediate feeding in response to glucose deficit are C1 CA neurons.

Adrenal medullary-mediated hyperglycemia is of major importance for rapid restoration of blood glucose in response to acute glucose deficit. Adrenal medullary epinephrine promotes glucagon secretion, inhibits insulin secretion, and acts directly on the liver and white adipose tissue to mobilize stored glucose and also fatty acids. The presence in the VLM of spinally projecting CA neurons necessary for the adrenal medullary hyperglycemic response to glucoprivation has been recognized for some time (19, 22, 32–37). The present results indicate that selective CNO-induced activation of these spinally projecting CA neurons is sufficient to produce adrenal

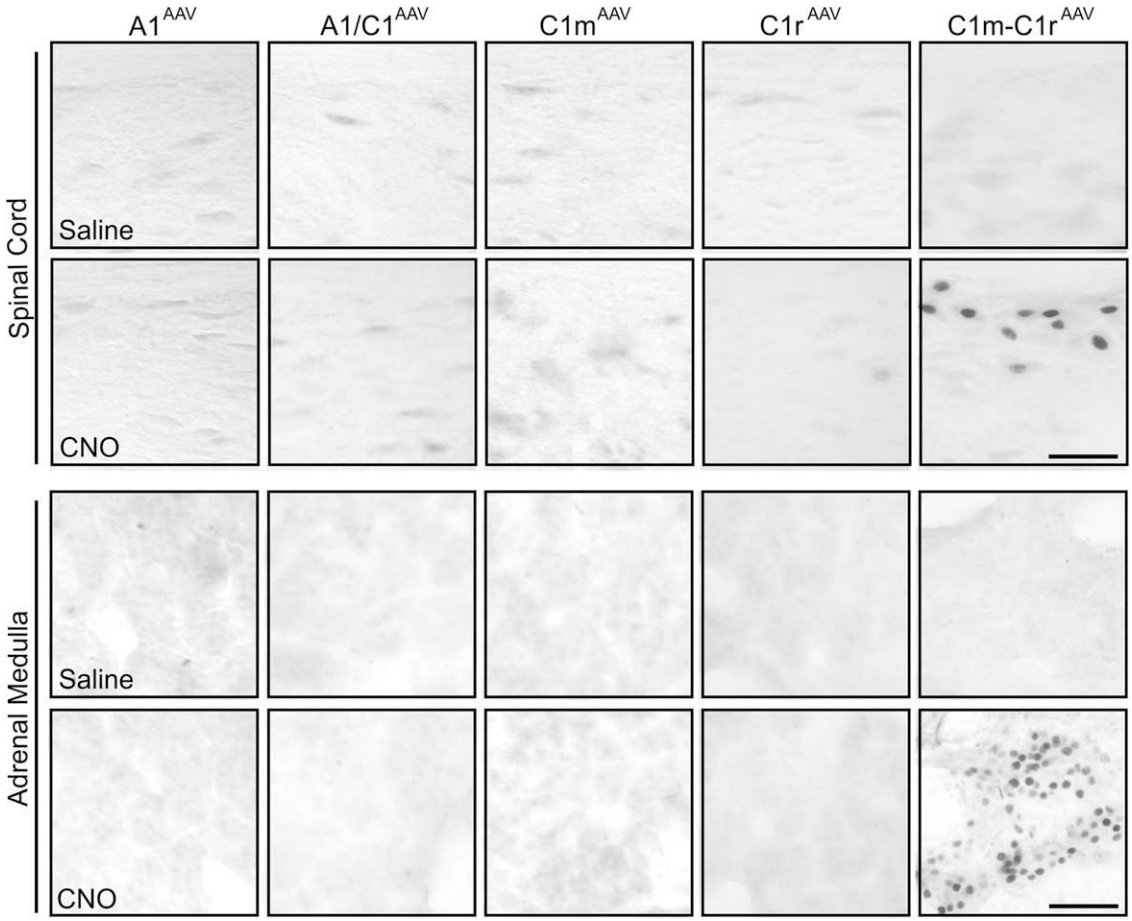

Figure 7. Expression of c-Fos in spinal cord and adrenal medulla in virus-transfected Th-Cre^{+} rats. Representative images of c-Fos expression in (upper) spinal segment T6 and (lower) adrenal medulla in A1$^{AAV\text{-}hM3D}$, A1/C1$^{AAV\text{-}hM3D}$, C1m$^{AAV\text{-}hM3D}$, C1r$^{AAV\text{-}hM3D}$, and C1m+C1r$^{AAV\text{-}hM3D}$ rats 2 hours after saline or CNO (1 mg/kg intraperitoneal) injection. Scale bar = 50 μm.

medullary c-Fos expression and hyperglycemia in the absence of glucoprivation, confirming their fundamental role in adrenal medullary activation. Our results might also indicate that the C1 neurons controlling adrenal medullary secretion are more widely distributed along the longitudinal extent of C1r and C1m than previously thought, overlapping considerably with the neurons controlling food intake and, to a lesser extent, those controlling corticosterone secretion. That stimulation of feeding and corticosterone required transfection of only one C1 site but stimulation of blood glucose responses required transfection of two adjacent sites might have resulted from a more diffuse distribution of blood glucose control within the VLM.

It has become clear that, in addition to the differences in their projection targets, the functionally distinct populations of the C1 neurons mediating feeding and blood glucose responses differ in other ways as well, including the signaling mechanisms that activate them. Specifically, glucosamine and alloxan (both glucokinase inhibitors), phloridzin (a sodium-linked glucose transporter antagonist), and 5TG (an antiglycolytic agent), all increase feeding when injected intraventricularly (38–42). However, only 5TG, injected into these same sites, increases blood glucose (43). Moreover, we have shown that these agents increase feeding in a CA-dependent manner regardless of whether injected into the lateral or fourth ventricle (43). Therefore, future investigations are expected to reveal additional phenotypic differences between these CA neuronal subgroups that reflect their distinct physiological roles in glucoregulation.

Corticosterone secretion contributes importantly to glucose counterregulation. Among its other actions, corticosterone promotes peripheral amino acid mobilization, hepatic gluconeogenesis, reduced insulin sensitivity, increased usage of fatty acids, and reduced glycolysis (5–9). These effects of corticosterone secretion are associated with a rapid shift in metabolic substrate usage that increases and preserves glucose availability to the brain (44). However, it is important to note that these actions are not responsible for the rapid elevation of glucose that occurs in response to an acute glucose deficit. The latter hyperglycemic response is mediated by adrenal

medullary epinephrine secretion and is eliminated by adrenomedullary denervation (32, 33). In addition, hypothalamic DSAP injections that reduce the corticosterone response to glucoprivation do not impair the adrenomedullary hyperglycemic response (13).

Previous neurochemical data strongly support a role for CA neurons in stimulating corticosterone secretion in response to some stressors (29, 30, 45–47). Hypothalamic CRH neurons are major innervation targets for C1 neuron axons (48). CA subpopulations within the C1 cell group coexpress NPY and/or the cocaine- and amphetamine-regulated transcript (CART) (31). Both NPY and CART are involved in control of corticosterone secretion. Of all NPY neurons in the brain, C1 neurons provide the largest percentage of NPY innervation to the PVH (mainly the parvocellular region) (30). Similarly, CRH neurons in the parvocellular PVH are densely innervated by terminal varicosities that contain the epinephrine biosynthetic enzyme, phenethanolamine-*N*-methyl transferase, and coexpress CART (49, 50). Currently, the relative importance of corelease of CA with NPY and/or CART is not known.

Previously, we demonstrated that nanoliter injections of 5TG into A1/C1 increased corticosterone secretion (15). We also demonstrated that corticosterone secretion in response to glucoprivation is impaired in rats in which hypothalamically projecting CA neurons are retrogradely ablated after hypothalamic DSAP treatment (13). In addition, a recent report has indicated that optogenetic stimulation of C1 CA neurons increases plasma corticosterone in DBH-Cre^{+} mice (51). Our present results, showing that activation of DREADD-transfected C1 neurons evokes corticosterone secretion in rats are consistent with these previous reports and collectively confirm the presence of a VLM to PVH CA pathway that increases corticosterone secretion in response to a glucose deficit. CNO injections most effectively triggered corticosterone secretion in rats with DREADD transfection of A1/C1 and C1m neurons, suggesting a relatively restricted distribution of CA neurons mediating this response. Retrograde lesions of hindbrain CA neurons by hypothalamic DSAP injections impair the corticosterone response to glucoprivation but not the circadian rhythm of corticosterone secretion or the response to swim stress (13). Therefore, it is possible that the corticosterone response elicited in the present study by CNO activation of VLM CA neurons is specifically related to glucoregulation. However, it is also possible that at least some CA neurons could elicit corticosterone secretion in response to inputs from neurons responsive to some nonglucoprivic stressors (37).

Pharmacogenetic activation of C1 neurons triggered downstream activation of neurons that receive CA neuron projections. For example, activation of C1 neurons resulted in increased c-Fos expression in the PVH. In addition, some non-CA neurons, but no A2 neurons, in the dorsal medulla were activated after CNO injection of A1/C1 DREADD-transfected rats. In addition to demonstrating activation of downstream targets, our results also indicate that A2 neurons are not excited by projections from VLM CA neurons. In fact, if A2 neurons do receive projections from A1 or C1 neurons within our transfection sites, these projections must be inhibitory.

None of the CRRs measured in our experiment were activated by CNO in rats in which A1 neurons had been transfected caudal to the A1/C1 group. Although this result encourages a focus on the role of C1 neurons in the activation of glucoprivic feeding, corticosterone secretion, and adrenal medullary responses, we could not conclude that the A1 neurons in the A1/C1 cluster do not contribute to these responses. Neurons throughout the extent of the A1 group respond to both glucoprivation and, after A1 DREADD transfection, to CNO. A1 neurons contribute to the noradrenergic innervation of hypothalamic magnocellular neurons in the supraoptic nucleus of the hypothalamus (4, 52–54) and are involved in a number of neuroendocrine responses that might not be directly related to glucoregulation. For example, we found previously that the same hypothalamic DSAP lesions that abolished insulin-induced food intake and corticosterone secretion also impaired the vasopressin response to hypovolemic hypotension. However, hypoglycemia did not stimulate vasopressin secretion in controls, indicating that at least some of these A1 neurons are controlled by nonglucoprivic signals (55), which is also true for C1 neurons (56).

Although responses to profound glucoprivation require hindbrain CA neurons, it is still not known whether glucoprivic signals activate these neurons directly or whether CA neurons are downstream of other glucose-sensitive cells. However, glucoprivic feeding and elevation of blood glucose can be elicited even in rats in which all connections between the forebrain and hindbrain have been severed by midcollicular decerebration (57–59). In addition, these responses can be elicited by fourth, but not lateral, ventricular administration of the antiglycolytic agent, 5TG, after acute blockade of the cerebral aqueduct (60). In addition, localized nanoliter injections of 5TG into specific hindbrain CA sites robustly stimulate these and other CRRs (12, 15). Therefore, glucose-sensing cells of sufficient potency to drive these reflex responses must be located in the hindbrain. However, it is also clear that critical interaction occurs between CA neurons and forebrain sites, which, in some cases, could be bidirectional. For example, it is well known that orexin stimulates feeding. However, we have shown that CA

Appendix. Antibody Table

Peptide/Protein Target	Name of Antibody	Manufacturer, Catalog No.	Species Raised in; Monoclonal or Polyclonal	Dilution Used	RRID
mCherry	mCherry antibody	ClonTech Laboratories, 632543	Mouse; monoclonal	1:1000 (IHC)	AB_2307319
DsRed	DsRed antibody	ClonTech Laboratories, 632496	Rabbit, polyclonal	1:1000 (IHC)	AB_10013483
TH	TH antibody	Millipore, AB152	Rabbit, polyclonal	1:5000 (IHC)	AB_390204
DBH	DBH antibody	Millipore, MAB308	Mouse; monoclonal	1:10,000 (IHC)	AB_2245740
c-Fos	c-Fos antibody	Santa Cruz Biotechnology, SC-52G	Goat; polyclonal	1:5000 (IHC)	AB_2629503

Abbreviations: AB, antibody; IHC, immunohistochemistry; RRID, Research Resource Identifier.

neurons activate orexin neurons during glucoprivation and in response to CNO in A1/C1 DREADD-transfected rats (26), but that retrograde lesion of CA neurons by PVH or lateral hypothalamic DSAP injection abolishes the feeding induced by either lateral or fourth ventricular injection of orexin (26, 27). Similarly, activation of orexin neurons stimulates a hyperglycemic response via an orexinergic lateral hypothalamus-to-VLM pathway (61), and optogenetic stimulation of the PVH elicits a hyperglycemic response by a PVH-to-VLM pathway (37). Possibly such interactions occur during glucoprivic conditions and under circumstances other than urgent glucoprivation to engage and coordinate appetitive responses such as food seeking to facilitate coordination of ongoing behaviors with anticipated or ongoing increases in glucose usage and, possibly, to expand the participation of hindbrain glucoregulatory mechanisms in multiple aspects of metabolic homeostasis. In brief, the signaling elements that activate CA neurons required for CRRs, the circuitry controlled by these neurons, and the mechanisms that maintain activation of the required circuitry during glucoprivation are important questions that require additional work.

In conclusion, the data we have reported show that selective activation of CA neurons in the C1 cell group is sufficient to activate three CRRs that are crucial for maintenance and/or restoration of blood glucose in the face of glucose deficit. Taken together with previous work showing that selective immunotoxin DSAP lesion of these neurons permanently abolishes all three of these responses to glucose deficit (13, 16, 19), our findings focus attention on VLM CA neurons as crucial mediators of CRRs. Finally, our results also are consistent with the hypothesis that CA neuron dysfunction might play a role in the pathogenesis of hypoglycemia-associated autonomic failure, a complication of insulin therapy (1, 10) in which protective and restorative responses to glucose deficit are impaired (62, 63).

Acknowledgments

Financial Support: This work was supported by Public Health Service Grants R01 DK 40498 and R01 DK 081496 (to S.R.).

Correspondence: Ai-Jun Li, MD, PhD, Department of Integrative Physiology and Neuroscience, College of Veterinary Medicine, Washington State University, Pullman, Washington 99164-7620. E-mail: aijun@wsu.edu.

Disclosure Summary: The authors have nothing to disclose.

References

1. Cryer PE. Hypoglycemia-associated autonomic failure in insulin-dependent diabetes mellitus. *Adv Pharmacol*. 1998;**42**:620–622.
2. Niijima A. Neural mechanisms in the control of blood glucose concentration. *J Nutr*. 1989;**119**(6):833–840.
3. Smith GP, Epstein AN. Increased feeding in response to decreased glucose utilization in the rat and monkey. *Am J Physiol*. 1969; **217**(4):1083–1087.
4. Cato RK, Flanagan LM, Verbalis JG, Stricker EM. Effects of glucoprivation on gastric motility and pituitary oxytocin secretion in rats. *Am J Physiol*. 1990;**259**(3 Pt 2):R447–R452.
5. Divertie GD, Jensen MD, Miles JM. Stimulation of lipolysis in humans by physiological hypercortisolemia. *Diabetes*. 1991; **40**(10):1228–1232.
6. Djurhuus CB, Gravholt CH, Nielsen S, Mengel A, Christiansen JS, Schmitz OE, Møller N. Effects of cortisol on lipolysis and regional interstitial glycerol levels in humans. *Am J Physiol Endocrinol Metab*. 2002;**283**(1):E172–E177.
7. Novelli M, Pocai A, Chiellini C, Maffei M, Masiello P. Free fatty acids as mediators of adaptive compensatory responses to insulin resistance in dexamethasone-treated rats. *Diabetes Metab Res Rev*. 2008;**24**(2):155–164.
8. Xu C, He J, Jiang H, Zu L, Zhai W, Pu S, Xu G. Direct effect of glucocorticoids on lipolysis in adipocytes. *Mol Endocrinol*. 2009; **23**(8):1161–1170.
9. Campbell JE, Peckett AJ, D'souza AM, Hawke TJ, Riddell MC. Adipogenic and lipolytic effects of chronic glucocorticoid exposure. *Am J Physiol Cell Physiol*. 2011;**300**(1):C198–C209.
10. McCrimmon RJ. Update in the CNS response to hypoglycemia. *J Clin Endocrinol Metab*. 2012;**97**(1):1–8.
11. Ritter S, Llewellyn-Smith I, Dinh TT. Subgroups of hindbrain catecholamine neurons are selectively activated by 2-deoxy-D-glucose induced metabolic challenge. *Brain Res*. 1998;**805**(1-2): 41–54.

12. Ritter S, Dinh TT, Zhang Y. Localization of hindbrain glucoreceptive sites controlling food intake and blood glucose. *Brain Res*. 2000;**856**(1-2):37–47.
13. Ritter S, Watts AG, Dinh TT, Sanchez-Watts G, Pedrow C. Immunotoxin lesion of hypothalamically projecting norepinephrine and epinephrine neurons differentially affects circadian and stressor-stimulated corticosterone secretion. *Endocrinology*. 2003; **144**(4):1357–1367.
14. Ritter S, Dinh TT, Li AJ. Hindbrain catecholamine neurons control multiple glucoregulatory responses. *Physiol Behav*. 2006;**89**(4): 490–500.
15. Andrew SF, Dinh TT, Ritter S. Localized glucoprivation of hindbrain sites elicits corticosterone and glucagon secretion. *Am J Physiol Regul Integr Comp Physiol*. 2007;**292**(5):R1792–R1798.
16. Ritter S, Li AJ, Wang Q, Dinh TT. Minireview: the value of looking backward: the essential role of the hindbrain in counterregulatory responses to glucose deficit. *Endocrinology*. 2011;**152**(11): 4019–4032.
17. Wrenn CC, Picklo MJ, Lappi DA, Robertson D, Wiley RG. Central noradrenergic lesioning using anti-DBH-saporin: anatomical findings. *Brain Res*. 1996;**740**(1-2):175–184.
18. Wiley RG, Kline RH IV. Neuronal lesioning with axonally transported toxins. *J Neurosci Methods*. 2000;**103**(1):73–82.
19. Ritter S, Bugarith K, Dinh TT. Immunotoxic destruction of distinct catecholamine subgroups produces selective impairment of glucoregulatory responses and neuronal activation. *J Comp Neurol*. 2001;**432**(2):197–216.
20. Emanuel AJ, Ritter S. Hindbrain catecholamine neurons modulate the growth hormone but not the feeding response to ghrelin. *Endocrinology*. 2010;**151**(7):3237–3246.
21. I'Anson H, Sundling LA, Roland SM, Ritter S. Immunotoxic destruction of distinct catecholaminergic neuron populations disrupts the reproductive response to glucoprivation in female rats. *Endocrinology*. 2003;**144**(10):4325–4331.
22. Madden CJ, Stocker SD, Sved AF. Attenuation of homeostatic responses to hypotension and glucoprivation after destruction of catecholaminergic rostral ventrolateral medulla neurons. *Am J Physiol Regul Integr Comp Physiol*. 2006;**291**(3):R751–R759.
23. Witten IB, Steinberg EE, Lee SY, Davidson TJ, Zalocusky KA, Brodsky M, Yizhar O, Cho SL, Gong S, Ramakrishnan C, Stuber GD, Tye KM, Janak PH, Deisseroth K. Recombinase-driver rat lines: tools, techniques, and optogenetic application to dopamine-mediated reinforcement. *Neuron*. 2011;**72**(5):721–733.
24. Paxinos GW, Watson C. *The Rat Brain in Stereotaxic Coordinates*, 6th ed. San Diego, CA: Elsevier Inc.; 2007.
25. Li AJ, Wang Q, Dinh TT, Simasko SM, Ritter S. Mercaptoacetate blocks fatty acid-induced GLP-1 secretion in male rats by directly antagonizing GPR40 fatty acid receptors. *Am J Physiol Regul Integr Comp Physiol*. 2016;**310**(8):R724–R732.
26. Li AJ, Wang Q, Davis H, Wang R, Ritter S. Orexin-A enhances feeding in male rats by activating hindbrain catecholamine neurons. *Am J Physiol Regul Integr Comp Physiol*. 2015;**309**(4): R358–R367.
27. Li AJ, Wang Q, Elsarelli MM, Brown RL, Ritter S. Hindbrain catecholamine neurons activate orexin neurons during systemic glucoprivation in male rats. *Endocrinology*. 2015;**156**(8): 2807–2820.
28. Li AJ, Wang Q, Dinh TT, Ritter S. Simultaneous silencing of Npy and Dbh expression in hindbrain A1/C1 catecholamine cells suppresses glucoprivic feeding. *J Neurosci*. 2009;**29**(1):280–287.
29. Sawchenko PE, Swanson LW. The organization of noradrenergic pathways from the brainstem to the paraventricular and supraoptic nuclei in the rat. *Brain Res*. 1982;**257**(3):275–325.
30. Sawchenko PE, Swanson LW, Grzanna R, Howe PR, Bloom SR, Polak JM. Colocalization of neuropeptide Y immunoreactivity in brainstem catecholaminergic neurons that project to the paraventricular nucleus of the hypothalamus. *J Comp Neurol*. 1985; **241**(2):138–153.
31. Parker LM, Kumar NN, Lonergan T, McMullan S, Goodchild AK. Distribution and neurochemical characterization of neurons in the rat ventrolateral medulla activated by glucoprivation. *Brain Struct Funct*. 2015;**220**(1):117–134.
32. Brodows RG, Pi-Sunyer FX, Campbell RG. Neural control of counter-regulatory events during glucopenia in man. *J Clin Invest*. 1973;**52**(8):1841–1844.
33. Gagner JP, Gauthier S, Sourkes TL. Descending spinal pathways mediating the responses of adrenal tyrosine hydroxylase and catecholamines to insulin and 2-deoxyglucose. *Brain Res*. 1985;**325**(1-2):187–197.
34. Rappaport EB, Young JB, Landsberg L. Effects of 2-deoxy-D-glucose on the cardiac sympathetic nerves and the adrenal medulla in the rat: further evidence for a dissociation of sympathetic nervous system and adrenal medullary responses. *Endocrinology*. 1982; **110**(2):650–656.
35. Morrison SF, Cao WH. Different adrenal sympathetic preganglionic neurons regulate epinephrine and norepinephrine secretion. *Am J Physiol Regul Integr Comp Physiol*. 2000;**279**(5): R1763–R1775.
36. Verberne AJ, Sartor DM. Rostroventrolateral medullary neurons modulate glucose homeostasis in the rat. *Am J Physiol Endocrinol Metab*. 2010;**299**(5):E802–E807.
37. Zhao Z, Wang L, Gao W, Hu F, Zhang J, Ren Y, Lin R, Feng Q, Cheng M, Ju D, Chi Q, Wang D, Song S, Luo M, Zhan C. A central catecholaminergic circuit controls blood glucose levels during stress. *Neuron*. 2017;**95**(1):138–152.e5.
38. Woods SC, McKay LD. Intraventricular alloxan eliminates feeding elicited by 2-deoxyglucose. *Science*. 1978;**202**(4373): 1209–1211.
39. Slusser PG, Ritter RC. Increased feeding and hyperglycemia elicited by intracerebroventricular 5-thioglucose. *Brain Res*. 1980;**202**(2): 474–478.
40. Ritter S, Murnane JM, Ladenheim EE. Glucoprivic feeding is impaired by lateral or fourth ventricular alloxan injection. *Am J Physiol*. 1982;**243**(3):R312–R317.
41. Ritter S, Strang M. Fourth ventricular alloxan injection causes feeding but not hyperglycemia in rats. *Brain Res*. 1982;**249**(1): 198–201.
42. Flynn FW, Grill HJ. Fourth ventricular phlorizin dissociates feeding from hyperglycemia in rats. *Brain Res*. 1985;**341**(2):331–336.
43. Li AJ, Wang Q, Dinh TT, Powers BR, Ritter S. Stimulation of feeding by three different glucose-sensing mechanisms requires hindbrain catecholamine neurons. *Am J Physiol Regul Integr Comp Physiol*. 2014;**306**(4):R257–R264.
44. Li AJ, Wang Q, Dinh TT, Wiater MF, Eskelsen AK, Ritter S. Hindbrain catecholamine neurons control rapid switching of metabolic substrate use during glucoprivation in male rats. *Endocrinology*. 2013;**154**(12):4570–4579.
45. Ruggiero DA, Ross CA, Anwar M, Park DH, Joh TH, Reis DJ. Distribution of neurons containing phenylethanolamine N-methyltransferase in medulla and hypothalamus of rat. *J Comp Neurol*. 1985;**239**(2):127–154.
46. Plotsky PM, Otto S, Sutton S. Neurotransmitter modulation of corticotropin releasing factor secretion into the hypophysial-portal circulation. *Life Sci*. 1987;**41**(10):1311–1317.
47. Plotsky PM, Cunningham ET Jr, Widmaier EP. Catecholaminergic modulation of corticotropin-releasing factor and adrenocorticotropin secretion. *Endocr Rev*. 1989;**10**(4):437–458.
48. Wittmann G, Liposits Z, Lechan RM, Fekete C. Origin of cocaine- and amphetamine-regulated transcript-containing axons innervating hypophysiotropic corticotropin-releasing hormone-synthesizing neurons in the rat. *Endocrinology*. 2005;**146**(7): 2985–2991.
49. Fekete C, Wittmann G, Liposits Z, Lechan RM. Origin of cocaine- and amphetamine-regulated transcript (CART)-immunoreactive innervation of the hypothalamic paraventricular nucleus. *J Comp Neurol*. 2004;**469**(3):340–350.

50. Füzesi T, Wittmann G, Liposits Z, Lechan RM, Fekete C. Contribution of noradrenergic and adrenergic cell groups of the brainstem and agouti-related protein-synthesizing neurons of the arcuate nucleus to neuropeptide-Y innervation of corticotropin-releasing hormone neurons in hypothalamic paraventricular nucleus of the rat. *Endocrinology*. 2007;**148**(11):5442–5450.
51. Abe C, Inoue T, Inglis MA, Viar KE, Huang L, Ye H, Rosin DL, Stornetta RL, Okusa MD, Guyenet PG. C1 neurons mediate a stress-induced anti-inflammatory reflex in mice. *Nat Neurosci*. 2017;**20**(5):700–707.
52. Cunningham ET Jr, Sawchenko PE. Anatomical specificity of noradrenergic inputs to the paraventricular and supraoptic nuclei of the rat hypothalamus. *J Comp Neurol*. 1988;**274**(1):60–76.
53. Baylis PH, Robertson GL. Vasopressin response to 2-deoxy-D-glucose in the rat. *Endocrinology*. 1980;**107**(6):1970–1974.
54. Baylis PH, Robertson GL. Rat vasopressin response to insulin-induced hypoglycemia. *Endocrinology*. 1980;**107**(6):1975–1979.
55. Dinh TT, Flynn FW, Ritter S. Hypotensive hypovolemia and hypoglycemia activate different hindbrain catecholamine neurons with projections to the hypothalamus. *Am J Physiol Regul Integr Comp Physiol*. 2006;**291**(4):R870–R879.
56. Guyenet PG, Stornetta RL, Bochorishvili G, Depuy SD, Burke PG, Abbott SB. C1 neurons: the body's EMTs. *Am J Physiol Regul Integr Comp Physiol*. 2013;**305**(3):R187–R204.
57. DiRocco RJ, Grill HJ. The forebrain is not essential for sympathoadrenal hyperglycemic response to glucoprivation. *Science*. 1979;**204**(4397):1112–1114.
58. Flynn FW, Grill HJ. Insulin elicits ingestion in decerebrate rats. *Science*. 1983;**221**(4606):188–190.
59. Darling RA, Ritter S. 2-Deoxy-D-glucose, but not mercaptoacetate, increases food intake in decerebrate rats. *Am J Physiol Regul Integr Comp Physiol*. 2009;**297**(2):R382–R386.
60. Ritter RC, Slusser PG, Stone S. Glucoreceptors controlling feeding and blood glucose: location in the hindbrain. *Science*. 1981; **213**(4506):451–452.
61. Korim WS, Llewellyn-Smith IJ, Verberne AJ. Activation of medulla-projecting perifornical neurons modulates the adrenal sympathetic response to hypoglycemia: involvement of orexin type 2 (OX2-R) receptors. *Endocrinology*. 2016;**157**(2): 810–819.
62. Sanders NM, Ritter S. Repeated 2-deoxy-D-glucose-induced glucoprivation attenuates Fos expression and glucoregulatory responses during subsequent glucoprivation. *Diabetes*. 2000;**49**(11): 1865–1874.
63. Sanders NM, Ritter S. Acute 2DG-induced glucoprivation or dexamethasone abolishes 2DG-induced glucoregulatory responses to subsequent glucoprivation. *Diabetes*. 2001;**50**(12): 2831–2836.